Supplemental Figures

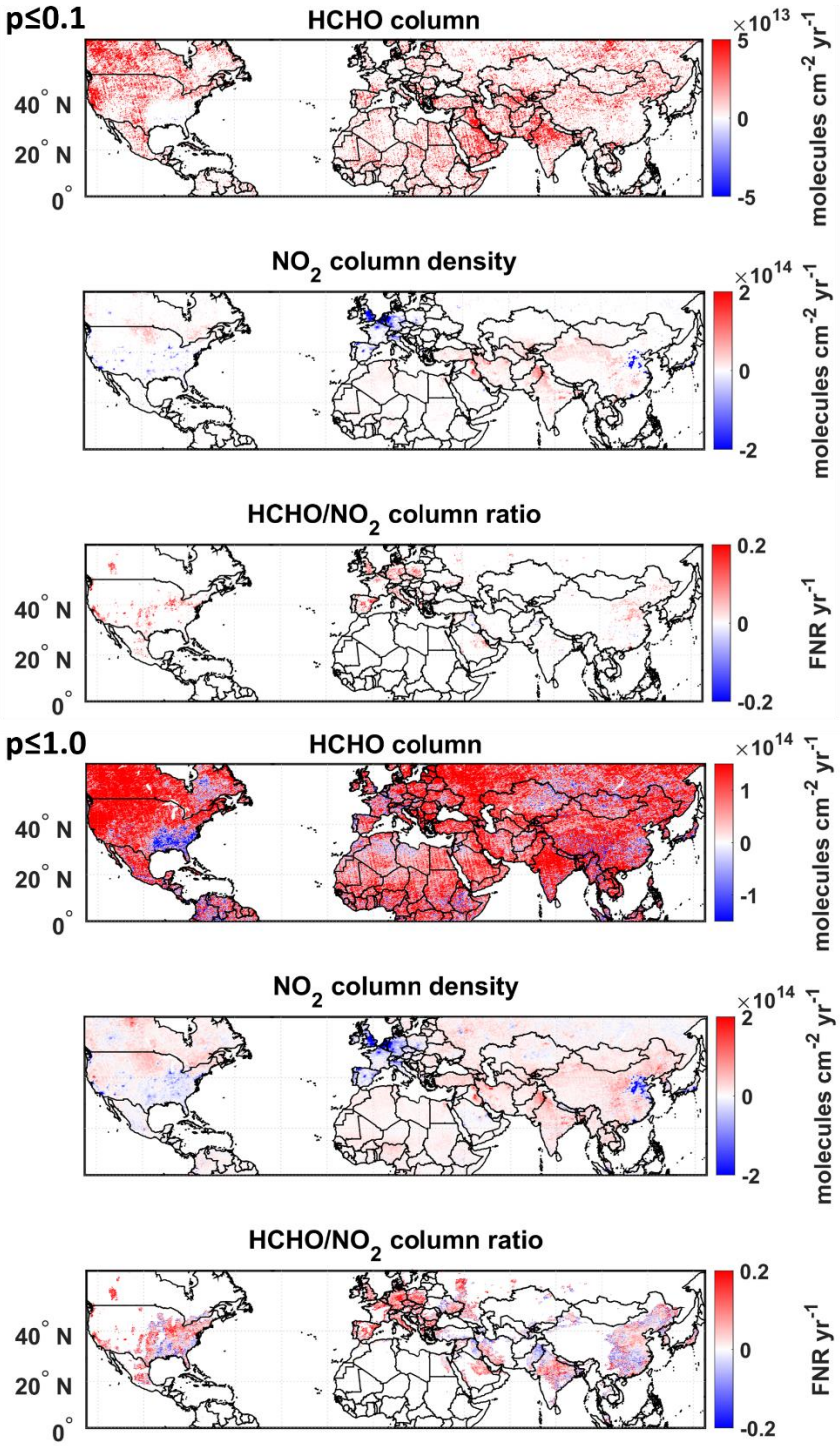

Figure S1. OMI-derived trends in summer mean (June-August) HCHO (top row) and NO_2 (middle row) VCDs (left column; units in molecule cm^{-2} yr^{-1}), and corresponding FNR values (bottom row; unitless yr^{-1}) at 0.1° × 0.1° latitude × longitude grid cells between 2005 and 2021. Values in the bottom row are displayed only for polluted regions (OMI NO_2 VCD > 1.2×10^{15} molecule cm^{-2}). The white color indicates data gaps or oceanic grid cells. All trend values that are displayed are at a 99% confidence level (top panels) and for all grid cells (bottom panels).

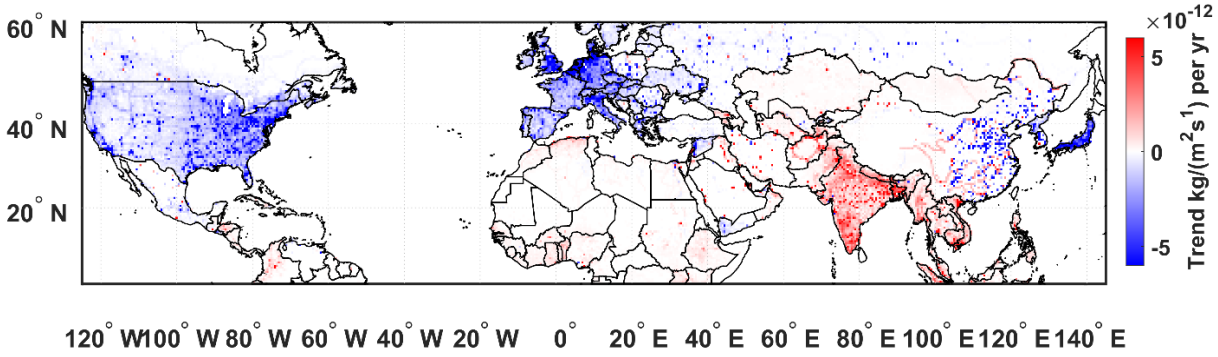

Figure S2. Trend in CEDS anthropogenic NO_x emission (kg m^{-2} s^{-2} yr^{-1}) between 2005-2019. Values are displayed for grids with statistically significant trends at a 95% ($p \leq 0.05$) confidence level.

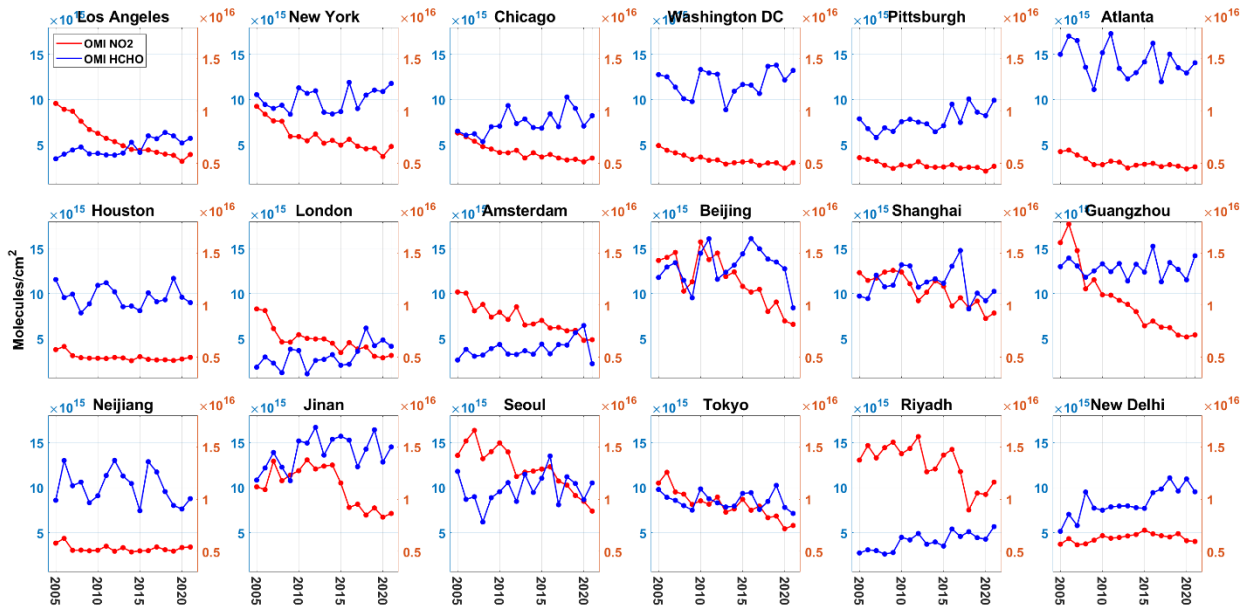

Figure S3. Time series of OMI-derived summer mean (June-August) VCD NO_2 and HCHO abundances (molecules cm^{-2}) for 18 selected cities across the North Hemisphere from 2005 to 2021.

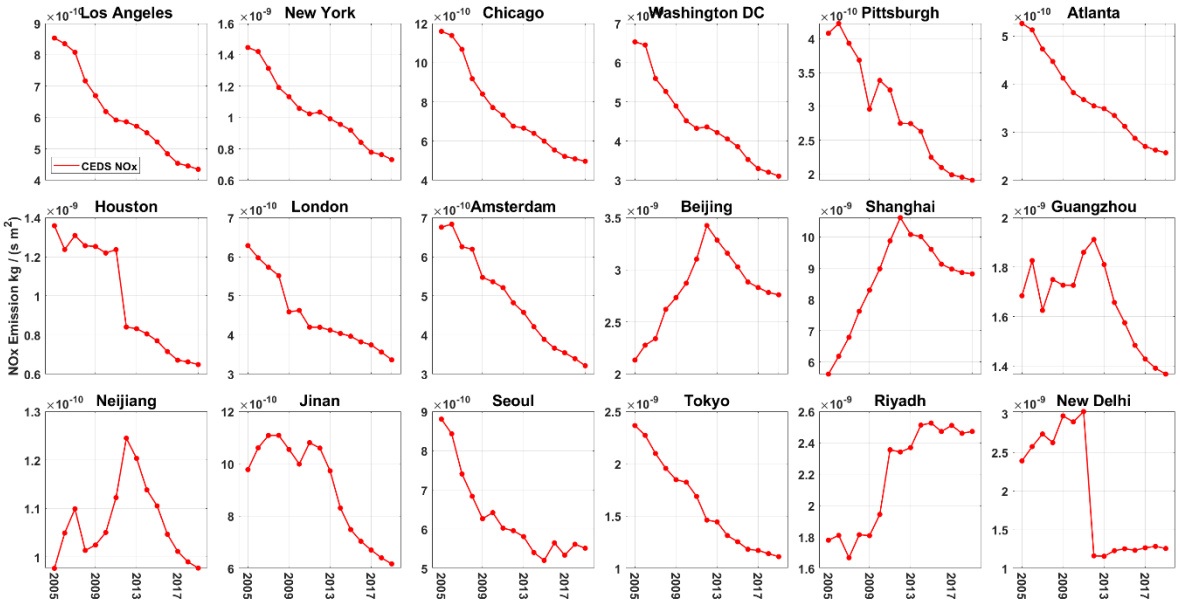

Figure S4. Time series of CEDS summer mean (June-August) anthropogenic NO_x emissions (kg NO_x s^{-1} m^{-2}) for 18 selected cities across the North Hemisphere from 2005 to 2019.